PRAMANA
— journal of
physics

Vol. 70, No. 3
March 2008
pp. 535–541

Gd-substituted Bi-2223 superconductor

D R MISHRA
Government Post Graduate College, Berinag, Pithoragarh, Uttaranchal, India and
National Physical Laboratory, New Delhi 110 012, India
E-mail: dr_devraj_mishra@yahoo.co.in

MS received 30 June 2006; revised 2 February 2007; accepted 8 June 2007

Abstract. The effects of gadolinium doping at calcium site on the normal and superconducting properties of Bi-2223 system were studied. The Gd-doped (BiPb)-2223 series of specimens, namely Batch I, II and III were sintered at three different sintering temperatures 830, 850 and 895°C respectively. The properties investigated are (1) the normal state resistivity with a view to study metal-to-insulator transition, (2) the XRD patterns of the specimens with a view to study the relative composition of (BiPb)-2212 and (BiPb)-2223 phases and (3) the superconducting fluctuation behaviour (SFB) with a view to determine the effect of doping, if any, on the dimensionality of the fluctuation conductivity of the system. The normal state resistivity of Gd-substituted Bi-2223 specimens shows metallic, semiconducting and insulating behaviour. The $T_c(R = 0)$ values indicate that (BiPb)-2223 phase is responsible for the observed superconducting transitions in Batch I and Batch II specimens with Gd concentrations $x \leq 0.7$. This observation is further confirmed in the analysis of XRD patterns of these specimens. Gadolinium, being a magnetic impurity, has pair breaking effect near the Fermi level and decreases $T_c(R = 0)$. The analysis of the superconducting fluctuation behaviour (SFB) shows a 2D dimensionality without any cross-over.

Keywords. High T_c superconductors; rare earth impurities; normal state resistivity; transition temperature variations; crystal growth.

PACS Nos 74.25.Fy; 74.62.Dh; 74.72.Hs; 76.30.Kg

1. Introduction

It is well-known that a CuO-based superconductor, in general, behaves like a Mott–Hubbard insulator at low carrier concentrations, like a superconductor with a semiconducting normal state resistivity behaviour at intermediate carrier concentrations and like a superconductor with a typical metallic normal state resistivity behaviour at sufficiently high carrier concentrations. Common high T_c superconducting systems such as YBCO and BSCCO are no exceptions. Different aliovalent substitutions or changes in the oxygen stoichiometry are known to alter the carrier concentration, leading to significant changes in the normal state resistivity behaviour and significant changes in the normal state transport behaviours and simultaneously influence the superconducting critical temperature T_c.

Various researchers, who have studied the effect of doping in Bi-based high-T_c superconductors, seem to support the above discussion. Substitution of Pr and Ce at Ca^{2+} sites in (BiPb)-2212 system causes T_c depression due to aliovalent Pr, Ce (3+, 4+) substitutions [1]. This substitution affects the normal state resistivity at sufficiently high dopant concentrations and causes a metal–insulator transition.

Pr substitution at Ca sites in (BiPb)-2223 system not only leads to a T_c depression but also to the formation of (BiPb)-2212 phase [2]. The normal state resistivity and its temperature dependence is a function of Pr concentrations. The substitution of Ce at Ca sites in BSCCO (2212) single crystals shows that the lattice parameters a and b increase while c decreases with increasing Ce concentration [3].

Gadolinium substitution in BSCCO (2212) system for various doping levels [4] showed that the density of states at the Fermi level was reduced with increasing gadolinium ion contents at calcium sites. This study also shows that the vacuum annealing of the samples increased the critical temperature even at optimum hole concentration ($x = 0.1$). These studies [1–4] however, are incomplete, as the microscopic effects of substitution of Pr, Ce and Gd in the lattice in any of the above studies, are not discussed.

Previous reports suggest 2D superconducting fluctuation behaviour (SFB) in BSCCO (2212) system [5] and BSCCO (2223) system [5,6]. Other researchers [7,8] have also confirmed 2D superconducting fluctuation behaviour in BSCCO system. The analysis of SFB in $\Delta\sigma$ analysis for single crystal BSCCO (2212) system [9] however, shows a distinct 2D–3D cross-over. These studies [5–9] however, do not discuss the effect of substitution on superconducting fluctuation behaviour (SFB) in BSCCO systems. This paper summarises the effect of gadolinium doping at calcium site on the normal and superconducting properties of BPSCCO (2223) system. This study forms part of a detailed investigation on the substitutional effects of d- and f-band materials (see also [10,11]).

2. Experimental method

The specimens with nominal composition $Bi_{1.6}Pb_{0.4}Sr_2Ca_{2-x}Gd_xCu_3O_\delta$ ($x = 0$, 0.1, 0.2, 0.3, 0.4, 0.5, 0.6, 0.7, 0.8, 0.9 and 1.0) were prepared using the usual solid state reaction technique. All the chemicals used were of 4N purity. The appropriate quantities of the metal oxides and the carbonates were taken and thoroughly mixed. The calcination of the mixture after grinding was done at 800, 820 and 840°C for about 30 h each with intermediate repeated grindings. The calcined mixture was then palletized in rectangular and circular shapes and was finally sintered at three different temperatures. The specimens of Batches I, II and III were sintered respectively at temperatures 830, 850 and 895°C for 120 h each. Batch III specimens with $x \leq 0.4$ partially melted during sintering at 895°C. Most of the specimens, except the pure, undoped (BiPb)-2223, survived at 850°C. This is therefore, the maximum temperature for the sintering of the complete series of gadolinium-substituted (BiPb)-2223 specimens. The specimens, after sintering, were furnace cooled to the ambient temperature.

The specimens were characterised for their phase purity by X-ray diffractrometry using a Siemen's D-500 diffractometer with CuK_α radiation. The DC resistivity measurements were carried out using standard four-probe method in an

APD cryocooler over a temperature range of 12–300 K. The estimated accuracy of the resistivity measurement is $\pm 10^{-8}$ Ohm-cm. The accuracy for the temperature measurement is ± 0.01 K.

3. Results and discussion

3.1 *Normal state resistivity; metal-to-insulator transition*

The formation of 2223 phase in the pure BiSrCaCuO specimen is an extremely slow process [12]. The formation of a liquid phase in $(BiPb)_2Sr_2Ca_2Cu_3O_\delta$ composed of Ca_2PbO_4, Sr_2PbO_4 or a eutectic of 2201 and Ca_2PbO_4 [13], however, improves the mobility of ions leading to its rapid growth. All gadolinium-substituted specimens except the pure, undoped one, survived at 850°C. This indicates that gadolinium substitution, unlike V or Nb substitutions [10,11], has suppressed this process. The possibility of the substituents occupying the interstitial or substitutional sites in the crystal structure and of getting precipitated out is small if the final sintering of the specimens is carried out at 830°C, a temperature lower than 850°C. The focus of this study, therefore, is the observations on Batch II specimens and the observations on Batch I and Batch III specimens, are being studied in reference to these observations.

Table 1[1] shows batch denomination, specimen composition, sintering conditions (temperature and time duration), and T_c values for various specimens. Batch I, II and III, as discussed in the previous section, correspond to different final sintering temperatures.

The resistivity vs. temperature (ρ–T) plots for specimens of Batch I, II, III are shown in figure 1. The normal state resistivity of pure Bi-2223 specimen and of the specimens with low gadolinium concentrations shows metallic behaviour. It, however, is almost independent of the temperature for specimens, especially of Batch II, of higher gadolinium concentrations, i.e., $x \cong 0.6$–0.7. This semiconducting behaviour indicates that the term (B/T) in Anderson–Zou relationship [15] is dominant at these concentrations. This shows that gadolinium substitution causes a decrease in the carrier concentration of the BSCCO system. Specimens of Batch I and Batch II with gadolinium concentration $x \leq 0.7$ show superconducting transition. Figures 2a and 2b show the plots of $T_c(R = 0)$ values against the Gd concentration x, for Batch I and Batch II specimens respectively.

Sanada *et al* [4] have shown that the specimens with gadolinium substituted at calcium site in (BiPb)-2212 system are superconducting upto a Gd concentration of 0.4 atomic percent. The transition temperature $T_c(R = 0)$ values for specimens of Batches I and II with Gd concentration $x \leq 0.4$ are different from the reported values [4] of the transition temperatures for Gd-substituted (BiPb)-2212 specimens. The specimens of Batches I and II with $x > 0.4$ are superconducting, which is also

[1]For tables 1–2 and figures 1–5, see http://www.ias.ac.in/pramana/v70/p535/supplement.pdf

different from the reported result on the corresponding Gd-substituted (BiPb)-2212 specimens [4]. This shows that (BiPb)-2223 phase is responsible for the observed superconducting transitions in specimens with $x \leq 0.7$. Therefore, gadolinium substitution decreases the transition temperature but does not inhibit the formation of (BiPb)-2223 phase. These observations are further confirmed by the XRD spectra of these specimens, as, is discussed later.

The $T_c(R = 0)$ values of the melted specimens of Batch III, which were sintered at 895°C, however, match with those reported for Gd-substituted (BiPb)-2212 specimens [4]. This is because (BiPb)-2223 phase in Batch III specimens decomposes due to partial melting and leads to the formation of (BiPb)-2212 phase.

The specimens with gadolinium concentration $x \geq 0.8$ for Batches I and II, however, do not show any sign of superconducting transition. It suggests that both (BiPb)-2223 and (BiPb)-2212 phases are Mott insulators for these Gd-doping levels. The Batch III specimens are insulators for $x \geq 0.7$.

Figure 3 shows the XRD spectra of Batch II specimens with $x = 0$, 0.2, 0.4, 0.6, 0.8 and 1.0. Here peaks corresponding to different phases are shown as BiPb(2223) $\rightarrow \blacktriangle$, BiPb(2212) $\rightarrow \bullet$, and BiPb(2201) $\rightarrow +$. The analysis of these spectra shows that undoped specimen consists of almost pure (BiPb)-2223 phase. It also confirms the presence of peaks corresponding to (BiPb)-2223 in the specimens with $x \geq 0.4$. The (BiPb)-2223 phase, as suggested by $T_c(R = 0)$ values, is in fact, responsible for the observed superconducting transition in specimens of Batches I and II with gadolinium concentration $x \leq 0.7$. The XRD patterns of specimens with still higher gadolinium concentration $x \geq 0.8$, show that (BiPb)-2212 is the dominant phase in these specimens.

An analysis of (BiPb)-2223 and (BiPb)-2212 composition and the relative stability of the latter for higher Gd concentration can be had from the relative peak intensities of prominent phases in the XRD pattern. Figure 4 shows the variation of the normalised or relative peak intensities of prominent peaks belonging to (BiPb)-2223 and (BiPb)-2212 phases plotted against the gadolinium concentration. The peak intensities have been normalised with respect to 0012H reflections. Here, L and H stand for (BiPb)-2212 and (BiPb)-2223 phases respectively. The peaks 002H, 0012H, 115H and 119H that correspond to (BiPb)-2223 phase, in general, show an increase with increasing Gd concentration. Peaks 117L and 113L that correspond to (BiPb)-2212 appear only in specimens with higher concentrations of gadolinium, i.e. for $x = 0.8$ and 1.0. Therefore, it can be concluded here that the presence of low concentrations of gadolinium ($x < 0.8$) at calcium site does not inhibit the growth of (BiPb)-2223 phase.

The lattice constants of the Gd-substituted specimens of Batch II were evaluated from the XRD patterns of these specimens. The lattice constants of the pure specimen are: $a = b = 5.408$ Å, $c = 37.08$ Å. Gadolinium in Gd^{3+} state has been substituted at Ca site in (BiPb)-2223 phase and the ionic radii of Ca^{2+} and Gd^{3+} are comparable. Therefore, no significant change in the lattice parameters of the (BiPb)-2223 phase was observed. However, the normal state resistivity behaviour and $T_c(R = 0)$ values confirm the gadolinium substitution in these specimens.

The XRD patterns of the specimens with Gd-doping in Bi-2223 system are similar to the Pr-substituted specimens [2]. The comparative study of XRD patterns of Gd- and Pr-substituted specimens, however, shows that the specimens with Pr $\geq$

0.2 were predominantly composed of (BiPb)-2212 phase similar to the observations here, however, for a higher gadolinium concentration $x > 0.7$. Therefore, the formation of (BiPb)-2212 phase in Pr-substituted specimens has taken place at a lower Pr concentration ($x = 0.2$).

The rate of decrease of $T_c(R = 0)$ values in Pr-substituted (BiPb)-2223 is roughly 5 K/(%Pr) [2] as compared to 12 K/(%Gd) in Gd-substituted (BiPb)-2223. This difference is because, the ionic radii of Gd (3+ state) with co-ordination numbers of six and eight are 0.938 Å and 1.06 Å respectively, and are smaller compared to those of Pr, which are 1.09 Å and 1.14 Å respectively. Therefore, Gd has higher solubility in (BiPb)-2223 as compared to Pr, and is, more detrimental to the superconductivity. This further adds to the fact that gadolinium is a magnetic f-band element with high net magnetic moment. Gadolinium, therefore, like other magnetic impurities, disturbs the antiferromagnetic ordering in Cu–O planes and leads to pair-breaking effects near the Fermi level (see, for example, [10,11] and the references therein).

3.2 *Superconducting fluctuation behaviour (SFB) studies*

Thermodynamic fluctuations of the superconducting order parameter give rise to short-lived Cooper pairs at temperatures above the superconducting transition temperature T_c and cause rounding of the resistance vs. temperature curve near T_c. The study of superconducting fluctuation behaviour (SFB) provides information about the dimensionality of these thermodynamic fluctuations.

The superconducting fluctuation conductivity, $\Delta\sigma = \sigma_m - \sigma_n$, also known as paraconductivity is the difference of the measured normal state electrical conductivity σ_m close to T_c and the conductivity σ_n (often called the background conductivity), which is the expected conductivity in the absence of the thermodynamic fluctuations.

The background conductivity σ_n is determined by extrapolating the ρ–T curve for $T \gg T_c$ to T_c. This extrapolation is done by either using the linear relation of Aslamazov–Larkin (AL) model [14]

$$\rho(T) = a + bT \tag{1}$$

or by using Anderson and Zou (AZ) model [15]

$$\rho(T) = AT + B/T. \tag{2}$$

The constants a, b were determined by the best fit of eq. (1) to the experimental data. Similarly the constants A, B were determined by the best fit of eq. (2) to the same experimental data.

These determined values of a, b for AL model and A, B for AZ model for the pure, undoped (BiPb)-2223 specimen (sintered at 830°C) and Batch II Gd-substituted (BiPb)-2223 specimens (sintered at 850°C) are shown in table 2.

The fluctuation conductivity $\Delta\sigma$ is given by $\Delta\sigma = \sigma_{\text{measured}} - \sigma_{\text{calculated}} = 1/\rho_{\text{measured}} - 1/\rho_{\text{calculated}}$ where σ_{measured}, $\sigma_{\text{calculated}}$ are the measured and calculated conductivities and ρ_{measured}, $\rho_{\text{calculated}}$ are the measured and calculated

resistivities of the specimen. The calculated resistivity $\rho_{\text{calculated}}$, as discussed earlier, was evaluated graphically by the extrapolation of the resistivity (ρ) vs. temperature (T) or ρ–T curve in the region $T \gg T_c$ to T_c, using eqs (1) and (2) with corresponding constants a, b or A, B evaluated as above.

The reduced temperature ε is then given by $\varepsilon = (T - T_c)/T_c$. Here T_c for each specimen was determined graphically by plotting the rate of variation of resistivity with temperature $\mathrm{d}\rho/\mathrm{d}T$ against temperature T. The peak of $\mathrm{d}\rho/\mathrm{d}T$ vs. T curve corresponds to T_c (onset) value of the specimen.

The critical exponent λ in eq. (3), viz.

$$\frac{\Delta\sigma}{\sigma_{\text{RT}}} = A\varepsilon^{\lambda} \tag{3}$$

is, then given by the slope of the $\log(\Delta\sigma/\sigma_{\text{RT}})$ vs. $\log\varepsilon$ curve. Figure 5 shows the exemplary linear fit to $\log(\Delta\sigma/\sigma_{\text{RT}})$ vs. $\log\varepsilon$ curve, in accordance with the AL model, for the pure, undoped specimen sintered at 830°C. The critical exponent λ for this specimen was determined as -0.987 or -0.99.

The dimensionality of the thermodynamic fluctuations in the order parameter D is then evaluated using the relationship

$$D = 2(2 + \lambda). \tag{4}$$

The values of critical exponent λ for Batch II specimens are shown in table 2. It was observed that the values of critical exponent λ are in the range -0.91 to -1.26 and are scattered around $\lambda \sim -1.0$. Therefore, the fluctuations in the order parameter or the superconducting fluctuation behaviour (SFB) of gadolinium-substituted BPSCCO specimens has a 2D dimensionality. This result is in agreement with the previous reportings on BSCCO system [5–8]. However, the cross-over reported in ref. [9] was not observed.

4. Conclusions

The sintering of Gd-substituted (BiPb)-2223 specimens is possible at a temperature, at least 20°C higher than the melting temperature of the pure, undoped (BiPb)-2223 specimen. The $T_c(R = 0)$ values on comparison with the reported values for (BiPb)-2212 specimens [4] suggest that (BiPb)-2223 is the main phase responsible for the superconductivity upto gadolinium concentration $x \leq 0.7$. The analysis of the XRD patterns confirms that (BiPb)-2212 phase has formed only in the specimens with higher gadolinium concentrations $x \geq 0.8$. Gadolinium, a magnetic impurity like V, Nb [10,11] contributes towards the pair breaking effects and lowers T_c. Finally, 2D superconducting fluctuation behaviour (SFB) is present in the Gd-substitued (BiPb)-2223 specimens, in conformity with the previous reports on BSCCO system.

Acknowledgements

I gratefully acknowledge the help of Dr (Mrs) R Rajput in obtaining XRD patterns of the specimens. I am thankful to Prof. (retd) P N Dheer and Dr R G Sharma

for useful discussions. I am also thankful to CSIR and NPL for providing financial support (senior research fellowship) and facilities for the work to be carried out.

References

[1] V P S Awana, S K Agarwal, A V Narlikar and M P Das, *Phys. Rev.* **B48**, 1211 (1993)
[2] Rajvir Singh, Anurag Gupta, S K Agarwal, D P Singh and A V Narlikar, *Supercond. Sci. Technol.* **11**, 311 (1998)
[3] A Thamizhavel, D Prabhakaran, R Jayavel and C Subramaniam, *Physica* **C275**, 279 (1997)
[4] N Sanada, T Nakadaira, M Shimomura, Y Suzuki, Y Fukuda, M Nagoshi, Y Syono and M Tachiki, *Physica* **C263**, 286 (1996)
[5] F Vidal, J A Veira, J Maza, J J Ponte, F Alvarado, E Moran, J Amador, C Cascales, A Castro, M T Casais and I Rasines, *Physica* **C156**, 807 (1988)
[6] W Schnelle, E Braun, H Broicher, H Weiss, H Geus, S Ruppel, M Galffy, W Braunisch, A Waldorf, F Seidler and Wohlleben, *Physica* **C161**, 123 (1989)
[7] G Balestrino, A Nigro and R Vaglio, *Phys. Rev.* **B39**, 12264 (1989)
[8] J A Veira and F Vidal, *Phys. Rev.* **B42**, 8743 (1990)
[9] P Mandal, A Poddar, A N Das, B Ghosh and P Choudhary, *Physica* **C169**, 43 (1990)
[10] D R Mishra, P L Upadhyay and R G Sharma, *Physica* **C304**, 293 (1998)
[11] D R Mishra, S V Sharma and R G Sharma, *Parmana – J. Phys.* **54(2)**, 317 (2000)
[12] S Nhien and G Desgardin, *Physica* **C272**, 309 (1996)
[13] Jun Takada, Y Ikada and M Takamo, in: *Bismuth-based high-temperature superconductors* edited by Hiroshi Maeda, Kazumasa Togano (Marcel Dekker, USA, 1996), Chap. 5, p. 93
[14] L G Aslamazov and A I Larkin, *Phys. (Kyoto)* **30**, 897; *Phys. Lett.* **A26(6)**, 238 (1968); *Phys. Lett.* **A67(3)**, 226 (1978)
[15] P W Anderson and Z Zou, *Phys. Rev. Lett.* **60**, 132 (1988)

Supplementary page

Table 1. Batch denomination, sample composition, sintering conditions (temperature and time duration) and T_c values.

Batch denomination	Sample composition	x	Sintering temperature (°C) and time (h)	T_{co} (K)
Batch I	$Bi_{1.6}Pb_{0.4}Sr_2Ca_2Cu_3O_\delta$	0.0	830°C × 120 h	102.6
	$Bi_{1.6}Pb_{0.4}Sr_2Ca_{1.9}Gd_{0.1}Cu_3O_\delta$	0.1	830°C × 120 h	79.7
	$Bi_{1.6}Pb_{0.4}Sr_2Ca_{1.7}Gd_{0.3}Cu_3O_\delta$	0.3	830°C × 120 h	82.2
	$Bi_{1.6}Pb_{0.4}Sr_2Ca_{1.4}Gd_{0.6}Cu_3O_\delta$	0.6	830°C × 120 h	32.4
	$Bi_{1.6}Pb_{0.4}Sr_2Ca_{1.0}Gd_{1.0}Cu_3O_\delta$	1.0	830°C × 120 h	–
Batch II	$Bi_{1.6}Pb_{0.4}Sr_2Ca_2Cu_3O_\delta$	0.0	850°C × 120 h	–
	$Bi_{1.6}Pb_{0.4}Sr_2Ca_{1.9}Gd_{0.1}Cu_3O_\delta$	0.1	850°C × 120 h	80.3*
	$Bi_{1.6}Pb_{0.4}Sr_2Ca_{1.8}Gd_{0.2}Cu_3O_\delta$	0.2	850°C × 120 h	84.6
	$Bi_{1.6}Pb_{0.4}Sr_2Ca_{1.7}Gd_{0.3}Cu_3O_\delta$	0.3	850°C × 120 h	81.8
	$Bi_{1.6}Pb_{0.4}Sr_2Ca_{1.6}Gd_{0.4}Cu_3O_\delta$	0.4	850°C × 120 h	66.4
	$Bi_{1.6}Pb_{0.4}Sr_2Ca_{1.5}Gd_{0.5}Cu_3O_\delta$	0.5	850°C × 120 h	55.0
	$Bi_{1.6}Pb_{0.4}Sr_2Ca_{1.4}Gd_{0.6}Cu_3O_\delta$	0.6	850°C × 120 h	34.2
	$Bi_{1.6}Pb_{0.4}Sr_2Ca_{1.3}Gd_{0.7}Cu_3O_\delta$	0.7	850°C × 120 h	15.5
	$Bi_{1.6}Pb_{0.4}Sr_2Ca_{1.2}Gd_{0.8}Cu_3O_\delta$	0.8	850°C × 120 h	–
	$Bi_{1.6}Pb_{0.4}Sr_2Ca_{1.1}Gd_{0.9}Cu_3O_\delta$	0.9	850°C × 120 h	–
	$Bi_{1.6}Pb_{0.4}Sr_2Ca_{1.0}Gd_{1.0}Cu_3O_\delta$	1.0	850°C × 120 h	–
Batch III	$Bi_{1.6}Pb_{0.4}Sr_2Ca_2Cu_3O_\delta$	0.0	895°C × 120 h	*
	$Bi_{1.6}Pb_{0.4}Sr_2Ca_{1.9}Gd_{0.1}Cu_3O_\delta$	0.1	895°C × 120 h	25.0*
	$Bi_{1.6}Pb_{0.4}Sr_2Ca_{1.8}Gd_{0.2}Cu_3O_\delta$	0.2	895°C × 120 h	14.4*
	$Bi_{1.6}Pb_{0.4}Sr_2Ca_{1.6}Gd_{0.4}Cu_3O_\delta$	0.4	895°C × 120 h	29.0
	$Bi_{1.6}Pb_{0.4}Sr_2Ca_{1.5}Gd_{0.5}Cu_3O_\delta$	0.5	895°C × 120 h	12.8
	$Bi_{1.6}Pb_{0.4}Sr_2Ca_{1.4}Gd_{0.6}Cu_3O_\delta$	0.6	895°C × 120 h	–

*Melted specimens

Table 2. Sample composition, T_c values, a, b, A, B parameters and the critical exponent λ values for the pure (BiPb)-2223 specimen (sintered at 830°C) and the Batch II specimens (sintered at 850°C).

Gadolinium concentration x	$T_c(R=0)$ values	Parameters				Critical exponents	
		a	b	A	B	λ_{AL}	λ_{AZ}
0.0	102.6	0.00123	6.37E-06	9.8E-06	0.1027	−0.99	−1.03
0.1	80.3	0.00138	6.47E-06	9.91E-06	0.11206	−1.00	−0.97
0.2	84.6	9.74E-04	6.56E-06	9.17E-06	0.07585	−1.13	−1.12
0.3	81.8	0.00241	7.2E-06	1.33E-05	0.20677	−1.05	−0.90
0.4	66.4	0.00482	1.06E-05	2.24E-05	0.43671	−1.06	−1.20
0.5	55	0.00995	1.04E-05	3.43E-05	0.9487	−0.96	−1.14
0.6	34.2	0.02828	−4.54E-07	7.23E-05	2.50501	−0.98	−0.91
0.7	15.5	0.04308	−3.8E-05	8.18E-05	3.3516	−1.20	−1.26
0.8	–	0.06395	−4.2E-05	8.45E-05	8.170	–	–
0.9	–	0.11154	−1.2E-04	1.08E-04	13.980	–	–
1.0	–	0.11555	−1.4E-04	9.6E-05	14.169	–	–

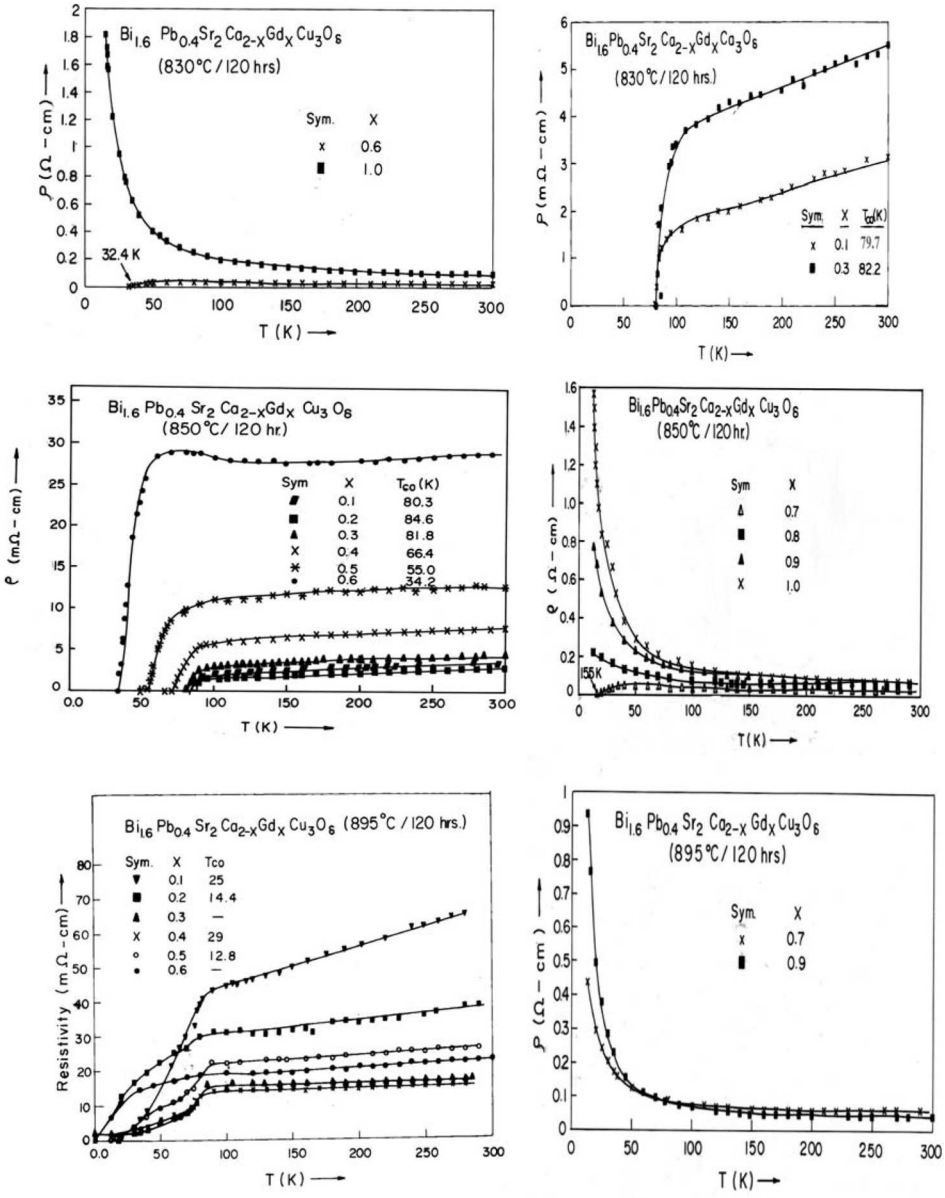

Figure 1. Resistivity vs. temperature curves for gadolinium-substituted BPSCCO samples (Batch I, II and III). Batch III samples $x \leq 0.4$ (bottom-left) were molten deformed pieces.

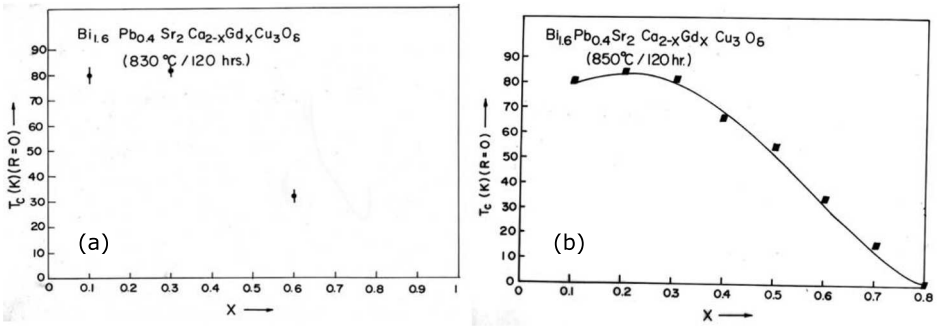

Figure 2. Curve showing the variation of $T_c(R = 0)$ values with gadolinium concentration for (**a**) Batch I and (**b**) Batch II samples.

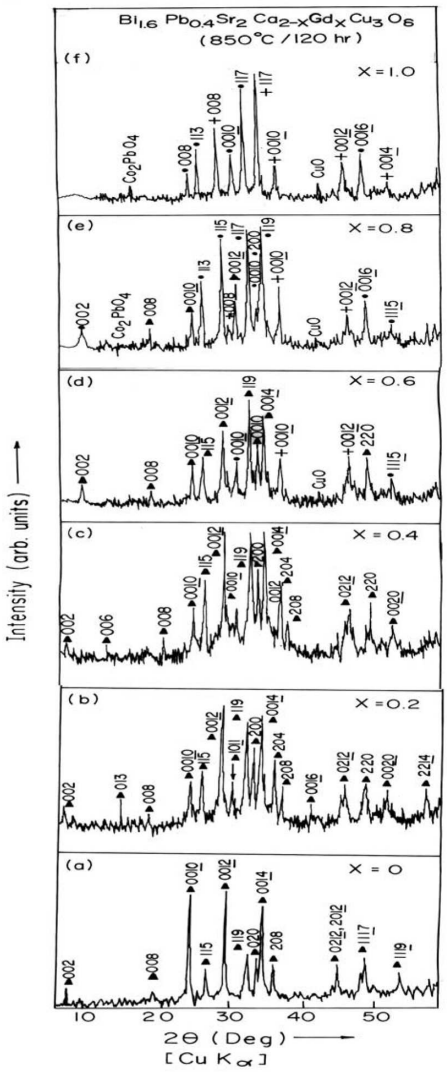

Figure 3. X-ray diffraction pattern for $Bi_{1.6}Pb_{0.4}Sr_2Ca_{2-x}Gd_xCu_3O_\delta$ ($x = 0$, 0.2, 0.4, 0.6, 0.8, 1.0). Peaks corresponding to different phases are shown as BiPb(2223) → ▲ , BiPb(2212) → •, and BiPb(2201) → +.

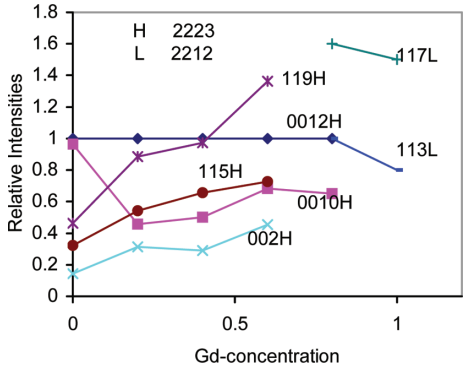

Figure 4. The relative peak intensities of (BiPb)-2223 and (BiPb)-2212 phases (normalised relative to 0012H peak). Peaks 117L and 113L appeared only in higher concentrations of gadolinium. (Here L and H stand for (BiPb)-2212 and (BiPb)-2223 phases respectively.)

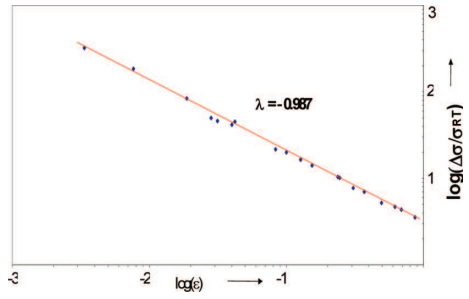

Figure 5. Linear fit to $\log(\Delta\sigma/\sigma_{\mathrm{RT}})$ vs. $\log\varepsilon$ curve, in accordance with the AL model, for the pure, undoped specimen sintered at 830°C (log has been taken to the base 10).